

NATURAL CONVECTION ON A VERTICAL STRETCHING SURFACE WITH SUCTION AND BLOWING

Shankar Goud B^a, Ratna Kumari Jilugu^{b,*}, Gayathri Bharadwaj^c

^aDepartment of Mathematics, JNTUH College of Engineering Hyderabad, Kukatpally-85, Telangana state, India

^b02 Electrical Machines, BHEL Ramachandrapuram, Hyderabad-32, Telangana state, India

^cDepartment of Mechanical Engineering, JNTUH College of Engineering Hyderabad, Kukatpally-85, Telangana state, India

*Email: bsgoud.mtech@gmail.com, ratna.227@gmail.com, gayathribharadwaj.b@gmail.com

In this paper, the natural convective heat transfer from a stretching sheet oriented vertically involving surface mass transfer is of primary focus. A similarity solution in three dimensions is described for energy and momentum. The transformed equations are solved by using MATLAB bvp4c in-built numerical solver. For a set out of Prandtl numbers and surface mass transfer rates, friction factor and Nusselt numbers are tabulated. Heat transfer mechanism is observed to have an influence by surface mass transfer.

Keywords: Stretching sheet, Heat transfer, Natural convention, steady flow, friction factor.

1. Introduction

There are many practical applications of the viscous fluid flow study involving heat transfer due to stretching surface in the fields of manufacturing where plastic and rubber sheets are blown a gaseous medium through the unsolidified material. Other notable applications of the study are spinning of fibres, Extrusion processes, continuous coating and glass blowing. This was noted by some of the researchers viz., Surma Devi et.al [1] deliberate on 3-dimensional, unsteady boundary-layer flow due to a stretching surface. Heat and mass transfer flows on a stretching sheet in the existence of suction or blowing was studied by [2, 5, 7, 9, 15, 17] but radiation effect [19], chemical reactive effect considered [20]. Heat and mass transfer on MHD boundary layer flows and on shrinking sheet with suction was studied by Battacharyya [3 & 4]. MHD viscous boundary layer flow over a stretching sheet and flat surfaces was studied by [6, 10, 13]. Also similar research but considering heat flux was studied by [11]. BSGoud and Rajashekar [12, 16 & 21] have studied the Finite element solution effects on unsteady MHD boundary layer flow past a parabolic started vertical plate with viscous dissipative, mass diffusion, variable temperature and source/suction [21]. Bestman [14] investigated on free convection boundary layer flow in a porous medium with suction and mass transfer. Heat generation effects on natural convection boundary-layer over a vertical porous flat plate in a porous medium were studied by [18].

The current work is about natural convective heat transfer in an incompressible, 3-dimensional steady flow past a stretching sheet involving blowing and suction. Using Boussinesq assumptions, a 3-dimensional similarity solution to the Navier-Stokes equations are described. The governing equations are renovated into coupled nonlinear ordinary differential equations by using the MATLAB tool, i.e., in-built bvp4c numerical solver.

2. Mathematical Formulation

For this study, consider an incompressible, steady fluid flowing with a velocity bx past a plane stretching perpendicular to the x – direction. Also consider that the y -axis of sheet makes an angle α with the horizontal and z – axis of sheet is normal to the sheet. Components of velocity are given by ' u ' in x direction, ' v ' in y direction and ' w ' in z direction. Figure 1 can be used as a reference for flow model and coordinate system. Let us neglect effects along the edges and hence all the variables along the y – direction are independent. Therefore the Boussinesq approximation governing equations are:

Momentum:

$$\frac{\partial u}{\partial x} + \frac{\partial w}{\partial z} = 0 \quad \dots (1)$$

$$u \frac{\partial u}{\partial x} + w \frac{\partial w}{\partial z} = v \frac{\partial^2 u}{\partial x^2} + g \beta (T - T_\infty) \cos \alpha \quad \dots (2)$$

$$w \frac{\partial v}{\partial z} = v \frac{\partial^2 v}{\partial z^2} + g \beta (T - T_\infty) \sin \alpha \quad \dots (3)$$

$$w \frac{\partial w}{\partial z} = v \frac{\partial^2 w}{\partial z^2} - \frac{1}{\rho} \frac{\partial p}{\partial z} \quad \dots (4)$$

Energy:

$$w \frac{\partial T}{\partial z} = \frac{v}{Pr} \frac{\partial^2 T}{\partial z^2} \quad \dots (5)$$

The following are the boundary conditions to be applied

$$z = 0 : u = bx, v = 0, w = W, T = T_w$$

$$z \rightarrow \infty : u = 0, v = 0, \frac{\partial w}{\partial z} = 0, T = T_\infty$$

3. Coordinate Transform

The method of similarity solutions is used to reduce the independent variables by one or more. This is the most probably used method in fluid mechanics to obtain exact solutions. Ames [8] describes the methods for equations of physical interest for generating similarity transformations. In the field of limiting solutions the asymptotic solutions are used as similarity solutions. A physical insight into these details of complex fluid flows may be obtained by using similarity solutions for complex fluid flows. Most of the characteristics exhibited by these solutions describe the actual problem for the physical, dynamic and thermal parameter.

$$u = bx f'(\eta) + A \cos \alpha \psi(\eta), v = A \sin \alpha \phi(\eta), w = -\sqrt{b \nu \varphi}, \theta(\eta) = \frac{T - T_\infty}{T_w - T_\infty}, \eta = \sqrt{\frac{b}{\nu}}, A = \frac{g \beta (T_w - T_\infty)}{b} \quad \dots (6)$$

The above equations of (6) are substituted in (1)-(5) equations, then the following are the resultant equations:

$$f''' + ff'' - (f')^2 = 0 \quad \dots (7) \quad \theta'' + Pr f \theta' = 0 \quad \dots (8)$$

$$\phi'' + f \phi' + \theta = 0 \quad \dots (9) \quad \psi'' + f \psi' - \psi f' + \theta = 0 \quad \dots (10)$$

In the above equations, prime denotes differentiation with respect to η only. The transformed boundary conditions for the velocity and temperature fields are given by

$$f(0) = f_w, f'(0) = 1, \theta(0) = 1, \phi(0) = 0, \psi(0) = 0, \quad \dots (11)$$

$$f'(\infty) = 0, \theta(\infty) = 0, \phi(\infty) = 0, \psi(\infty) = 0$$

The mass transfer parameter $f_w = \frac{-W}{\sqrt{b \nu}}$ varies in sign for injection and surjection. It is -ve for injection and +ve for surjection.

The stretching surface undergoes shear stresses and are given by

$$\tau_{zx} = \mu \left. \frac{\partial u}{\partial z} \right|_{z=0} = \rho \sqrt{b \nu} [bx f''(0) + A \cos \alpha \psi'(0)] \quad \dots (12)$$

$$\tau_{zy} = \mu \left. \frac{\partial v}{\partial z} \right|_{z=0} = \rho \sqrt{b \nu} A \sin \alpha \phi'(0) \quad \dots (13)$$

The surface skin friction factors along x-axis and y-axis are

$$Cf_x = \frac{2\tau_{zx}(0)}{\rho(bx)^2} = \frac{2}{\sqrt{Re_x^2}} \left(-1 + \left(\frac{Gr_x}{Re_x^2} \right) \cos \alpha \cdot \psi'(0) \right) \quad \dots (14)$$

$$Cf_y = \frac{2\tau_{zy}(0)}{\rho(bx)^2} = \frac{2}{\sqrt{Re_x^2}} \left(\frac{Gr_x}{Re_x^2} \right) \sin \alpha \cdot \phi'(0) \quad \dots (15)$$

Where $Gr_x = \frac{x^3 g \beta (T_w - T_\infty)}{\nu^2}$, $Re_x = \frac{(bx)x}{\nu}$, Fourier law is used to write the heat flux at a point as

$$q_w = -K_f \left. \frac{\partial T}{\partial z} \right|_{z=0} = -K_f \sqrt{\frac{b}{\nu}} (T_w - T_\infty) \theta'(0). \quad \dots (16)$$

$$\text{The heat transfer coefficient at any point is given by } h = \frac{q_w}{(T_w - T_\infty)} \quad \dots (17)$$

The Nusselt number at any point may be written as

$$Nu_L = \frac{hL}{K_f} = -\sqrt{Re_L} \theta'(0) \quad \dots (18)$$

4. Numerical Solution and Discussion

In this part we use MATLAB solver to attain mathematical solutions for the differential equations which are non-linear applying boundary conditions. Wall friction and rate of heat transfer due to the varied mass transfer factor f_w is numerically exposed in Table 1. Injection increases friction factor and fall down the rate of heat transfer. Alternatively, suction decreases friction factor and enhances the rate of heat transfer.

Increased Prandtl number leads to an increased rate of heat transfer, decreased induced buoyancy flow and shear stress. This behaviour is clearly observed from the data in table 2, where there are no conditions of surface mass transfer. Figures 2 to 6 focus on surface mass transfer effects on temperature and velocity distributions. Velocity distribution component in z -direction is depicted in figure 2 where $Pr = 7.0$. There is a lot of influence of surface mass transfer value. A constant value $f(0)$ is approached by $f(\eta)$ monotonically such that $f'(\infty) = 0$. The numerical values of $f(\infty)$ are a measure of entrainment velocity. At the surface, higher board velocity is due to high suction velocity. Within the boundary layer, $f'(\infty)$ distribution is shown in figure 3. It can be clearly understood that more linear shape for $f'(\infty)$ is obtained by higher values of injection. Distribution of normalized temperature profiles for $Pr = 7.0$ is shown in figure 4 with varying surface mass parameter. Higher injection values thicken the thermal boundary layer. Alternative behaviour of thermal boundary layer is observed in case of higher suction and reduce of thermal boundary layer exponentially is observed in all specified cases. Maximum values of $\psi(\eta)$ (velocity factor of z -direction of normalized free convection) and $\phi(\eta)$ (velocity factor of y -direction in normalized free convection) are located far from the surface on increasing rate of injection. Figures 5 and 6 clearly depict the decrease of the velocity boundary layers in exponential manner. With an increased velocity level, suction is increased. Temperature gradient at the surface is steep on higher values of injection. This is amalgamated with a temperature reduction at the outer boundary region. The temperature is approximately equal to the ambient temperature as length increases. In case of rapid increase in ambient temperature with height, the body temperature increase due to heat transfer mechanisms and may not be able to achieve the local ambient temperature. When $\alpha = 0$, on a vertically stretched surface, equation 14 describes a zero shear stress $\frac{Gr_x}{Re_x^2} \psi'(0) = 1$. Zero shear stress or critical value of the boundary layer $\frac{Gr_x}{Re_x^2}$ is smaller for Prandtl numbers having lower value than the Prandtl numbers having higher values. For sample,

the value $\left(\frac{Gr_x}{Re_x^2} \right)_{crit}$ is 0.1740 at $Pr = 0.07$ where as its value is 10.79 at $Pr = 70$. For $\alpha \neq 0$, velocity is present in all the directions hence, in a rigid surface, there is no rise in induced natural convection in vertical direction. Alternatively, induced natural convection is slanted in the positive direction of y -axis, since $\phi(\eta)$ is larger than $\psi(\eta)$.

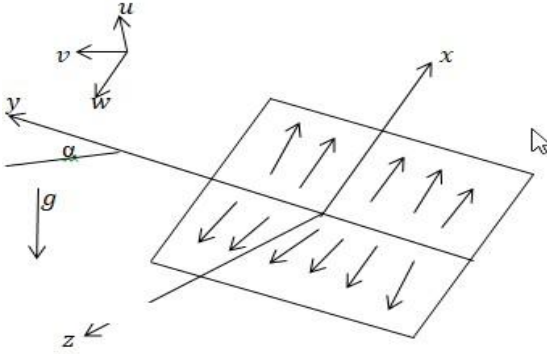


Figure:1. Flow model and directions.

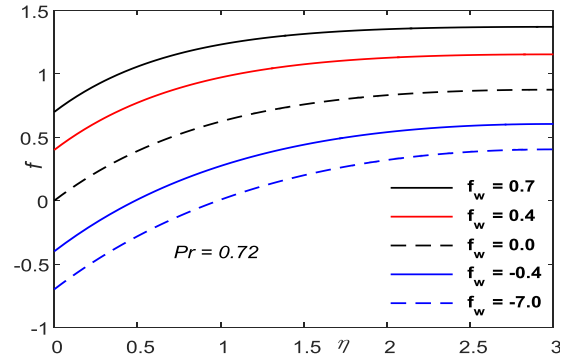


Figure 2: Stream function

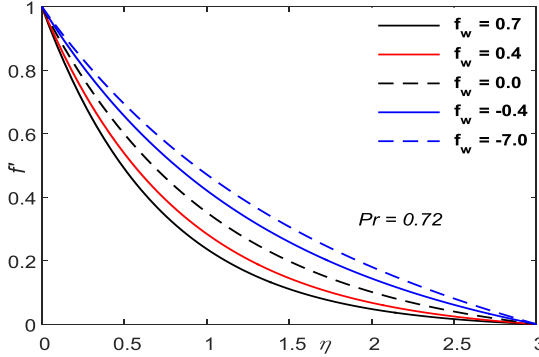


Figure 3. Distribution of $f'(\eta)$ within the boundary layer (velocity in z -direction).

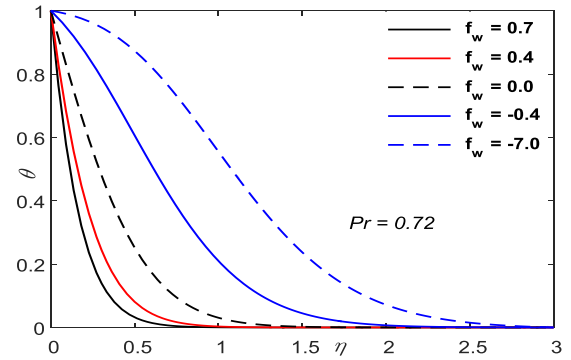


Figure 4. Temperature profiles.

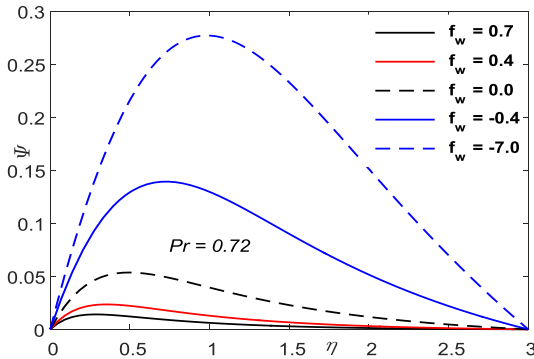


Figure5. Decrease of velocity boundary layers (velocity in z -direction).

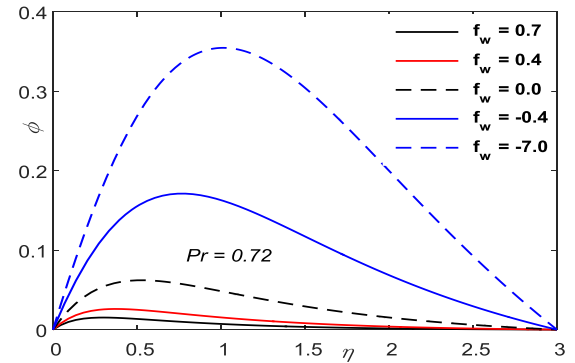


Figure .6. Decrease of velocity boundary layers (velocity in y -direction).

Table 1: The values of $f''(0), \theta'(0), \phi'(0), \psi'(0)$ for various values of mass transfer factors f_w for $Pr = 7.0$.

f_w	$f''(0)$	$\theta'(0)$	$\phi'(0)$	$\psi'(0)$
0.7	-1.418835	-5.799705	0.147772	0.142456
0.4	-1.231802	-3.989315	0.194900	0.185540
0.0	-1.014349	-1.890462	0.305539	0.281972
-0.4	-0.83420	-0.500116	0.507098	0.447013
-0.7	-0.722423	-0.087148	0.697118	0.589307

Table 2: The values of $f''(0), \theta'(0), \phi'(0), \psi'(0)$ for various values of Prandtl number for $f_w = 0$.

Pr	$f''(0)$	$\theta'(0)$	$\phi'(0)$	$\psi'(0)$
0.07	-1.014349	-0.352182	0.976804	0.822892
0.2	-1.014349	-0.388200	0.941902	0.795626
0.7	-1.014349	-0.534879	0.815210	0.696205
2.0	-1.014349	-0.911669	0.577967	0.507509
3.0	-1.014349	-1.159692	0.474313	0.423375
7.0	-1.014349	-1.890462	0.305539	0.281972
10	-1.014349	-2.303501	0.254389	0.237519
20	-1.014350	-3.349977	0.178888	0.170144
50	-1.014350	-5.424807	0.112816	0.109193
70	-1.014350	-6.458883	0.095310	0.092695

5. Conclusions

Free convection from a vertical stretching surface is analysed for the effects of surface mass transfer. The characteristics of flowing fluid and heat transfer are numerically computed for its dependence on Prandtl number and surface mass transfer. Tables are constructed for the missing values of thermal functions and velocity. Predictions on rate of heat transfer can be performed using this information. Also, surface friction factor can be estimated. Temperature field and flow field experience a higher influence by surface mass transfer. Higher entrainment velocity is observed at the surface due to suction. Linearity temperature profile and velocity profile is higher with injection. The thickness of thermal boundary layer is increased by injection and is alternatively reduced by surface suction as well as temperature and velocity profiles decay exponentially. Increase in Prandtl number, increases heat transfer rate. Decreasing the Prandtl number, thermal boundary layer's thickness is found to reduce leading to reduced resistance to heat transfer.

References

1. C. D. Surma Devi, H S. Takhar and G. Nath , Int. J. Heat mass transfer, 29(2), pp.1996-1999, 1986.
2. Gupta PS and Gupta AS., The Canadian Journal of Chemical Engineering, 55(6), pp.744 -746, 1977.
3. Krishnendu Bhattacharyya, Chemical Engineering Research Bulletin, 15, pp.12-17, 2011.
4. R. N. Jat ., Santosh Chaudhary, Applied Mathematical Sciences, 3(26), pp.1285 - 1294, 2009.
5. Vajravelu K , Journal of Mathematical Analysis and Applications, 188(3), pp. 1002-1011, 1994.
6. M. Fathizadeh, M. Madani, Yasir Khan, Naeem Faraz, Ahmet Yildirim, Serap., Tutkun, Journal of King Saud University - Science, 25(2), pp. 107-113, 2013.
7. Zailan Siri , Artisham Che Ghani., Ruhaila Md. Kasmani , BVP, 126, pp.1-16, 2018.
8. Ames, W.F., New York: Academic Press (1965).
9. J. E. Daskalakis, Canadian Journal of Physics, 70, pp. 1253–1260, 1993.
10. C. K. Chen and M. I. Char, J. of Mathematical Analysis and Applications, 135(2), pp.568-580, 1988.
11. M. Ferdows, Tania S. Khaleque, Bangalee, Int.j. Of heat and technology, 34(3), pp. 521-526, 2016.
12. B.Shankar Goud, Raja Shekar' *I-manager's Journal on Mathematics*, 7(1), pp.20-27, 2018.
13. Wang, C. Y [13]. J. of Applied Mathematics and Mechanics, 69(11), pp. 418–420, 1989.
14. A. R. Bestman, International Journal of Energy Research, 14(4), pp. 389–396, 1990.
15. M. Acharya, L. P. Singh, G. C. Dash, Int. Journal of Eng. Science, 37(2), pp. 189–211, 1999.
16. B.Shankar Goud., M.N Rajashekar, *Int. Research J. of Eng.and Technology*, 4(2), pp.471-47, 2017.
17. Ali, M. E, International Journal of Heat and Fluid Flow, 16(4), pp.280–290, 1995.
18. A. Postelnicu, T. Grosan, I. Pop, Int. Comm. Heat Mass Transfer, 27 (5) 729–738, 2000.
19. S. Shateyi, Journal of Applied Mathematics Volume 2008, Article ID 414830, 12 pages.
20. K. Bhattacharyya., G.C. Layek, Che. Engi.Communications, 197(12), pp.1527-1540, 2010.
21. B. Shankar Goud, MN Rajashekar. *IOSR Journal of Mathematics* , 12(6) Ver. IV, pp.55-64, 2016.